RSC Advances

PAPER

View Article Online
View Journal | View Issue

Cite this: *RSC Adv.*, 2017, **7**, 7483

Plasticizing and crosslinking effects of borate additives on the structure and properties of poly(vinyl acetate)†

Shiyu Geng,[a] Faiz Ullah Shah,[b] Peng Liu,[a] Oleg N. Antzutkin[bc] and Kristiina Oksman*[ad]

Received 22nd December 2016
Accepted 16th January 2017

DOI: 10.1039/c6ra28574k

www.rsc.org/advances

As an environmentally friendly, low-cost and widely used polymer, poly(vinyl acetate) (PVAc) is worth modifying to achieve better properties. Here, we report on the influence of borate additives on the structure and properties of partially hydrolysed PVAc. In addition to the general crosslinking function of borate additives, an extraordinary plasticizing effect was found. By controlling the pH from 4 to 11 during sample preparation, the plasticizing and crosslinking effects can be shifted. In alkaline conditions, the degree of crosslinking in the PVAc/borate sample is increased; however, this increase declines gradually with an increase in the borate additive content, which impacts the morphology of the PVAc latex particles, as well as the mechanical and thermal properties of the PVAc/borate films. In contrast, in acidic conditions, the PVAc/borate films are plasticized by borate additives; thus, their ultimate mechanical strength, elastic moduli and thermal stabilities decrease, while the water diffusivities increase.

Introduction

Poly(vinyl acetate) (PVAc) is a polymer that is widely used in many applications, such as paints, surface coatings, food additives and adhesives for wood, paper and cloth. PVAc, with its advantageous properties, can be considered a "green" material suitable for overcoming a range of environmental challenges. First, PVAc can be produced from renewable resources. Its monomer, vinyl acetate, can be synthesized from bioethanol, which is extracted from the biomass refining process, and then further treated by dehydration, oxidation and vinylation.[1] Second, PVAc is predominantly synthesized by emulsion polymerization, with the use of water as the dispersion medium during processing. This type of synthesis is a nontoxic, non-flammable and low-cost system, which is more environmentally friendly than other polymerization methods.[2–4] Finally, it has been reported that PVAc is principally biodegradable,[1] which means that it will be modified, hydrolysed, metabolized and finally assimilated by microbial organisms under specific conditions.

However, several drawbacks of PVAc, including deficient mechanical properties, a high water or humidity sensitivity and a poor performance at elevated temperatures,[5,6] pose limitations in some applications. During the last few decades, many studies have focused on improving the properties of PVAc. One of the most famous reports from 1940 by Perrin *et al.*[7] has described in detail, for the first time, copolymerization of ethylene with vinyl-acetate: The product poly(ethylene-*co*-vinyl-acetate) has then been widely used in various types of commercial products due to its much higher ductility and lower water sensitivity compared to pure PVAc. Recently, nanocomposites with improved properties achieved by adding nanosized reinforcements into PVAc, have received a great attention. Kaboorani *et al.* studied the effects of admixing of nanoclays and cellulose nanocrystals on the adhesive properties of PVAc, especially at elevated temperatures and in wet conditions.[5,6] Khan *et al.* improved the adhesive strength and toughness of PVAc dramatically by adding only 0.1 vol% of graphene.[8] Mathew *et al.* investigated the moisture absorption and its effect on the mechanical properties of PVAc reinforced by cellulose nanocrystals.[9] Gong *et al.* studied the viscoelastic properties and toughness of PVAc nanocomposites with cellulose nanofibers.[10,11]

Alternatively, crosslinking PVAc with certain crosslinkers, for instance, sodium tetraborate (borax), is another possible approach to enhance the mechanical and thermal properties and moisture resistance of PVAc. Borax, an environmentally benign mineral mined directly from the ground, is well known to crosslink diol-containing molecules in aqueous media under alkaline conditions and to form borate complexes. Many studies have been done on crosslinking of poly(vinyl alcohol) by borax

[a]*Division of Materials Science, Department of Engineering Sciences and Mathematics, Luleå University of Technology, SE-971 87, Luleå, Sweden. E-mail: kristiina.oksman@ltu.se*

[b]*Chemistry of Interfaces, Luleå University of Technology, SE-97187 Luleå, Sweden*

[c]*Department of Physics, University of Warwick, Coventry, UK*

[d]*Fibre and Particle Engineering, University of Oulu, Finland*

† Electronic supplementary information (ESI) available: ^{1}H NMR spectra of PVAc-4, PVAc-9.3 and PVAc-11 in DMSO-d_6; equation for calculation of PVAc hydrolysis degree; ^{13}C NMR spectra of PVAc-4, PVAc-9.3 and PVAc-11 in DMSO-d_6; solid-state ^{13}C CP-MAS NMR spectra of PVAc-4, PVAc-9.3 and PVAc-11; and toughness of each sample. See DOI: 10.1039/c6ra28574k

or its derivatives,[12–16] and crosslinking of partially hydrolysed PVAc to form gel-like materials has also been reported. Angelova *et al.* studied the structure and rheological properties of PVAc/borate gel after absorbing different organic liquids,[17,18] and this type of gel was further developed by Natali *et al.* for application as a cleaner for painted surfaces.[19]

In our previous research,[20] we combined both methods – reinforcing with nanocellulose and crosslinking with borax – to improve the properties of PVAc, and we found very interesting behaviour of borax-crosslinked PVAc films. Some experiments indicated that borate additives can not only provide crosslinking but also have a plasticizing effect on PVAc films prepared at specific pH, although this has not yet been fully explored. Thus, in this report, both plasticizing and crosslinking effects of borate additives on PVAc/borate samples prepared at different pH are investigated. The morphology of PVAc/borate latex particles as well as the structure, mechanical performance, thermal properties and moisture absorption behaviour of PVAc/borate films are explored. Furthermore, the relationship between the structure and properties of the PVAc/borate materials is also discussed in detail.

Experimental

Materials

Vinyl acetate monomer (99%) was purchased from Alfa Aesar, Karlsruhe, Germany. Potassium peroxodisulfate (KPS) was purchased from VWR International, Leuven, Belgium. Sodium hydroxide (pure pellets) and acetic acid (96%) were purchased from Merck KGaA, Darmstadt, Germany. Sodium tetraborate decahydrate (borax) (≥99.5%), glyceryl triacetate (GTA) (≥99%), docusate sodium salt (≥96%), and sodium bicarbonate (≥99.7%) were all purchased from Sigma-Aldrich, St. Louis, USA. All chemicals were used as received.

Sample preparation

Poly(vinyl acetate) (PVAc) was synthesized using an emulsion polymerization method, according to US patent 4812510.[21] Briefly, 2.25 g of docusate sodium salt as surfactant and 0.135 g of sodium bicarbonate were dissolved in 255 g of distilled water in a three-necked flask with a water-cooled condenser. The solution was heated to 353 K and kept under stirring. Then, 0.225 g of KPS, as an initiator of polymerization, and 2.25 g of vinyl acetate monomer were added. After 20 min, 42.75 g of vinyl acetate monomer was continuously fed into the flask dropwise over 3 h. Finally, the reaction was maintained at 353 K for another 30 min after feeding. The solid content of the obtained PVAc latex was 15.3 wt% and was measured by weighing before and after overnight drying in an oven at 333 K.

The compositions of the samples prepared in this study, with different borax content at various pH values, are given in Table 1. The PVAc/borate films were prepared by a crosslinking/plasticizing reaction, followed by solvent casting and hot pressing. The reaction for each sample was performed by adding a certain amount of a borax saturated solution (293 K) to the PVAc latex dropwise, and then, the pH of the dispersion was controlled to a selected value by sodium hydroxide (0.1 M) or acetic acid. Afterwards, the dispersion was heated at 353 K for 1 h with stirring, and then, the PVAc/borate latex was obtained. Next, GTA was added as a plasticizer and the weight ratio of GTA to PVAc in each sample was kept constant (GTA : PVAc = 5 : 95). Finally, the dispersion was poured into a Teflon Petri dish and dried in an oven with a fan at 313 K for 30 h. The dried film was peeled off and hot pressed using a laboratory press (LabEcon 300, Fontijne Grotnes, Netherlands) at 423 K for 1 min under a pressure of 1.1 MPa, with 2 min of pre-heating. The thickness of the obtained films was ~0.15 mm. The native PVAc latexes and dried films were prepared, with controlled pH values, as references, in the same manner as described above but without the addition of borax.

Table 1 Composition of all prepared PVAc and PVAc/borate materials, and their glass transition temperatures (T_g) and equilibrium moisture contents (M_e) (at 90% humidity, 293 K)

Sample coding	Borax content (wt% of dried film)	pH	T_g (K)	M_e (%)
PVAc-4	0	4	298.9	4.7 ± 0.5
X0.5PVAc-4[a]	0.5	4	298.3	5.6 ± 1.1
X1PVAc-4[a]	1	4	297.9	5.9 ± 1.2
X1.5PVAc-4[a]	1.5	4	297.5	5.9 ± 2.7
X2PVAc-4[a]	2	4	297.2	4.8 ± 1.1
X3PVAc-4[a]	3	4	296.8	6.7 ± 1.4
PVAc-9.3	0	9.3	298.7	8.6 ± 0.7
X0.5PVAc-9.3[a]	0.5	9.3	298.9	12.3 ± 1.4
X1PVAc-9.3[a]	1	9.3	299.3	15.9 ± 0.9
X1.5PVAc-9.3[a]	1.5	9.3	298.6	18.6 ± 3.0
X2PVAc-9.3[a]	2	9.3	297.6	11.9 ± 0.5
X3PVAc-9.3[a]	3	9.3	297.2	12.7 ± 1.5
PVAc-11	0	11	297.7	9.8 ± 0.8
X0.5PVAc-11[a]	0.5	11	298.2	19.7 ± 3.1
X1PVAc-11[a]	1	11	299.5	15.3 ± 1.1
X1.5PVAc-11[a]	1.5	11	299.8	21.6 ± 0.5
X2PVAc-11[a]	2	11	300.3	17.4 ± 3.3
X3PVAc-11[a]	3	11	298.9	15.2 ± 2.8

[a] Samples are coded as "XaPVAC-b", where "X" stands for the borax addition, "a" stands for borax content (wt%) in the samples and "b" stands for the controlled pH values during the sample preparation.

Characterization methods

Nuclear magnetic resonance (NMR) spectroscopy. All NMR spectra were recorded on a Bruker Ascend Aeon WB 400 NMR spectrometer. Liquid-state 400.21 MHz ^{1}H and 100.64 MHz ^{13}C NMR spectra were recorded in DMSO using standard Bruker pulse programs. Chemical shifts were expressed in parts per millions (ppm) from tetramethylsilane with the solvent resonance as the internal standard. Solid-state magic-angle-spinning (MAS) one-pulse NMR experiments (for ^{11}B and ^{13}C) or with cross-polarization (CP) from the protons and with proton decoupling were performed using a triple resonance HXY 4 mm MAS probe. The cross-polarization contact time was 4 ms in ^{13}C CP-MAS NMR experiments. The samples were packed in 4 mm standard ZrO_2 rotors. ^{11}B MAS NMR spectra were externally referenced using liquid samples of $Et_2O{\cdot}BF_3$ (0

ppm). ^{13}C chemical shifts were referenced to the least shielded resonance line of polycrystalline adamantine, used as the external standard (38.48 ppm relative to tetramethylsilane).[22] To prepare the native PVAc samples for NMR spectroscopy, the films were washed with distilled water for 24 h to remove the surfactant (docusate sodium salt) and the plasticizer (GTA) that may give additional signals in ^{13}C CP-MAS NMR spectra. The samples were then dried in the oven at 313 K. To prepare the dried borax powder as a reference material for ^{11}B MAS NMR, the pH of a 0.23 wt% borax aqueous solution was tuned to 11 with NaOH (0.1 M), and then, the solution was heated at 353 K for 1 h and dried in the oven to obtain a powder sample.

Atomic force microscopy (AFM) and scanning electron microscopy (SEM). AFM (Veeco MultiMode scanning probe with Bruker TESPA tips, USA) and SEM (Magellan 400 XHR-SEM, FEI Company, USA) were used for characterizing topography and morphology of the latex particles. The preparation of the AFM samples involved depositing one drop of diluted (0.01 wt%) aqueous solution of latex on freshly cleaved mica and drying at room temperature overnight. The samples were then analysed by tapping mode in AFM at *ca.* 303 K. The SEM samples were prepared in the same manner as for AFM and then coated with tungsten using a Bal-Tec MED 020 Coating system. The secondary electron images were captured at *ca.* 295 K.

Particle size measurements. The latex particle sizes of the samples were measured by a Zetasizer Nano ZS (Malvern, UK) with DTS0012 cells at 298 K. Each sample of the latex was diluted to 0.01 wt%, and 3 runs with 10 scans per run were processed for each measurement to determine the average value of the particle size.

Mechanical testing. A universal tensile testing machine Shimadzu AG-X (Kyoto, Japan) with an environmental chamber THC1-200SP and an SLBL-1kN load cell was used to measure the mechanical properties of the dried films. Materials were tested with 20 mm of gauge length and 5 mm min^{-1} of crosshead speed under 25% of humidity at 293 K. At least 5 specimens (5 × 40 mm) of each sample were tested, and the average was calculated. The elastic modulus was determined by the initial linear portion of the stress–strain curve, and the toughness, as work to fracture, was defined by the integrated area under the stress–strain curves.

Differential scanning calorimetry (DSC). A Mettler Toledo DSC 821^{e} with aluminium crucibles (ME-27331) was used for investigating the glass transition temperatures (T_g) of the samples (dried films) under nitrogen atmosphere. First, a blank curve was run to remove the background noise, and then, the samples were measured. In the first heating runs, all samples were heated from 233 K to 393 K, with a heating rate of 10 K min^{-1}, and then isothermal for 3 min to remove the heating history. Afterwards, the samples were cooled down rapidly with a cooling rate of 20 K min^{-1} and isothermal at 233 K for 3 min and then heated to 393 K again with the same heating rate (10 K min^{-1}) as in the first heating runs. The results from the second heating runs were considered, and T_g of the samples were determined by the middle points of the inclines between the extrapolated baselines.

Thermo-gravimetric analysis (TGA). The thermal stability of the dried films was studied by TGA using a Q500 analyser (TA Instruments, USA) with platinum sample pans. The tests were performed by temperature sweeps from room temperature to 873 K, with a heating rate of 10 K min^{-1} and nitrogen flow at 60 mL min^{-1}.

Moisture absorption measurement. The moisture absorption measurements procedure was performed according to the standard ASTM D 5229.[23] Briefly, 3 specimens (13 mm × 38 mm) of each sample (dried film) were dried in an oven at 318 K to remove the moisture until constant weights were reached, and then, they were placed into the thermostatic chamber with a controlled humidity of 90% at 293 K and weighed every 15 min until the moisture absorption reached equilibrium. The diffusivity of each sample was calculated by the average values of the three specimens based on the following equation:

$$D_z = \pi\left(\frac{h}{4M_e}\right)^2\left(\frac{M_2 - M_1}{\sqrt{t_2} - \sqrt{t_1}}\right)^2 \quad (1)$$

where h is the thickness of the sample, M_e is the equilibrium moisture content, and $(M_2 - M_1)/(\sqrt{t_2} - \sqrt{t_1})$ is the slope of the initial linear portion in the moisture absorption curve.

Results and discussion

Structure characterization

Chemical structure. In this work, all the materials (sample coding and compositions are shown in Table 1) with various borax content (from 0 to 3 wt%) were produced at pH 4, 9.3 or 11. Before investigating the effects of borate additives on the structure of PVAc, the basic structures of native PVAc (prepared without borax) as reference materials at pH 4, 9.3, and 11 were characterized by NMR spectroscopy. All three samples were slightly hydrolysed, and the degree of hydrolysis was calculated based on the integrals of acetate and methylene protons in liquid-state ^{1}H NMR spectra (see Fig. S1 in the ESI†). The data are summarized in Table 2. The solid-state ^{13}C MAS NMR spectra of these samples are illustrated in Fig. 1. The resonance

Table 2 The degree of hydrolysis and ^{13}C chemical shifts of –CHO carbons (region C) and –COO carbons (region D), as denoted in Fig. 1, of native PVAc films treated in various pH conditions

Sample coding	Hydrolysis degree (%)	^{13}C chemical shift (region C) (ppm)	^{13}C chemical shift (region D) (ppm)
PVAc-4	7.9	66.0	167.6
PVAc-9.3	9.8	67.3	170.4
PVAc-11	9.9	68.0	174.6

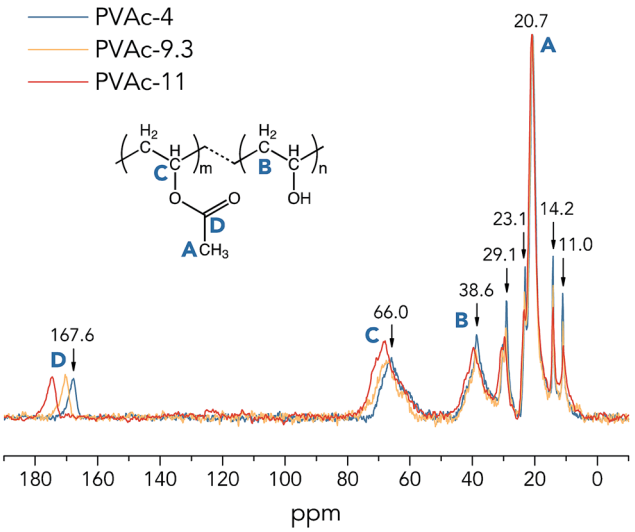

Fig. 1 One-pulse ^{13}C MAS NMR spectra of the native PVAc films (partially hydrolysed in various pH conditions).

lines assigned to $-CH_3$, $-CH_2$, –CHO and –COO carbons on the PVAc chains are labelled in these spectra by A, B, C and D, respectively. The resonance lines at 11.0 ppm, 14.2 ppm and 23.1 ppm were assigned to the methyl ($-CH_3$) carbons of the residual monomer or oligomer of vinyl acetate in the samples. In addition, the liquid-state ^{13}C NMR spectra in DMSO and the solid-state ^{13}C CP-MAS NMR spectra of the native PVAc samples are given in Fig. S2 and S3 in the ESI.†

From Fig. 1, it is clear that the ^{13}C sites of the native PVAc become more de-shielded (chemical shifts move towards higher ppm values) with an increase in pH from 4 to 11, especially for –CHO carbons (region C) and –COO carbons (region D), see Table 2. These spectral observations imply structural changes in PVAc-4, PVAc-9.3 and PVAc-11. Asakawa *et al.* investigated the hydrogen-bonding effect on ^{13}C NMR chemical shifts of L-alanine residues, and they found that carbon sites become more de-shielded with a decrease in length of hydrogen bonds.[24] Similarly, it is suggested here that an additional de-shielding of –CHO and –COO carbon sites in PVAc samples prepared in different pH conditions (see Fig. 1) is also caused by hydrogen bonding effects, as will be discussed in the following text. Table 2 shows that with an increase in pH, the degree of hydrolysis of PVAc is increased from 7.9% in PVAc-4 to 9.9% in PVAc-11, which indicates that there are larger numbers of hydroxyl groups present in PVAc-11, and thus, the polymer chains of PVAc-11 have a higher propensity to form hydrogen bonds with each other. A larger number of hydroxyl groups also contributes to a higher flexibility of the PVAc chains, because bulky acetate side groups (before the hydrolysis) cause larger restrictions in chain movement. As a result of a higher degree of hydrolysis in PVAc-11, polymer chains could pack more closely compared to those in PVAc-4 and generate more hydrogen bonds with a shorter length, which should cause a larger de-shielding of ^{13}C sites. Moreover, it is obvious that an additional de-shielding of resonance lines in regions C and D is significantly larger than that for other resonance lines (see Fig. 1), which implies that the –CHO and –COO carbon sites in PVAc are more strongly influenced by the pH compared with the methyl $-CH_3$ (region A) and methylene $-CH_2$ carbons (region B). This is because a larger number of the –CHO and –COO carbons are involved in the hydrogen bonds in the form of C–O–H···O and C=O···H–O, respectively,[25] and chemical shifts of these carbon sites are obviously more affected by hydrogen bonding compared to chemical shifts of methylene and methyl carbons, which are one more chemical bond further away from the hydrogen bond. However, it should be noted that the degree of hydrolysis of PVAc-9.3 (9.8%) is very close to that of PVAc-11 (9.9%), but according to NMR spectra in Fig. 1, there is an obvious difference in ^{13}C chemical shifts of corresponding carbon sites in these two samples. A possible reason is that polymer chains in PVAc-11 are shorter than in PVAc-9.3 due to a higher degree of cleavage in the harsher alkaline conditions.[26,27] Shorter chains have a higher mobility due to a less prominent entanglement effect in polymers,[28] that promotes the formation of a larger number of hydrogen bonds in PVAc-11 compared with PVAc-9.3, even though they have a similar degree of hydrolysis.

To further investigate the crosslinking effects of borate additives, solid-state ^{11}B MAS NMR spectra of dried borax powder and PVAc/borate materials were recorded and are illustrated in Fig. 2. From Fig. 2a, it can be seen that there are two types of boron sites present in the dried borax powder, one is tetra-coordinated boron [$B\varphi_4$] denoted in region A (approximately 1 ppm), and the other is tri-coordinated boron [$B\varphi_3$] shown in region B (approximately 15 ppm), where φ refers to either O or OH.[29] In Fig. 2b, one can see that there are two new resonance lines in the PVAc/borate samples in addition to regions A and B, which is attributed to the crosslinked tetra-coordinated boron species (region C, approximately 5 ppm) and exchanging boron atoms between boric acid and borate ions (region D, approximately 10 ppm), consistent with previous reports.[17]

The basic theory of crosslinking by borax has been introduced in detail in our previous work.[20] Here, the crosslinked borate fraction (f_c) and the absolute crosslinked borate content (n_a) of each sample out of the total amount of added borax were estimated from the integrated areas of the corresponding resonance lines in the ^{11}B MAS NMR spectra (Fig. 2b), and the results are tabulated in Table 3. We can see that f_c of the sample X1PVAc-9.3 (9.6%) is lower than that for X0.5PVAc-9.3 (16.9%), which illustrates that the conversion efficiency from original borax to the crosslinked borate is reduced with an increase in borax content at a certain pH level. Conversely, n_a of X1PVAc-9.3 (1.0×10^{-5} mol) is still larger than that in X0.5PVAc-9.3 (8.9×10^{-6} mol) due to a larger amount of the added borax. We can speculate that the increase in n_a will decline gradually as borax content is further increased as a result of the decreasing conversion efficiency. In addition, f_c of X1.5PVAc-11 (9.1%) is similar to that for X1PVAc-9.3 (9.6%), although the former sample contains more borax and n_a of X1.5PVAc-11 (1.5×10^{-5} mol) is the highest among the three samples in this study (see Table 3). Since the n_a is related to the total crosslinking degree of a PVAc/borate sample, it can be concluded that with an

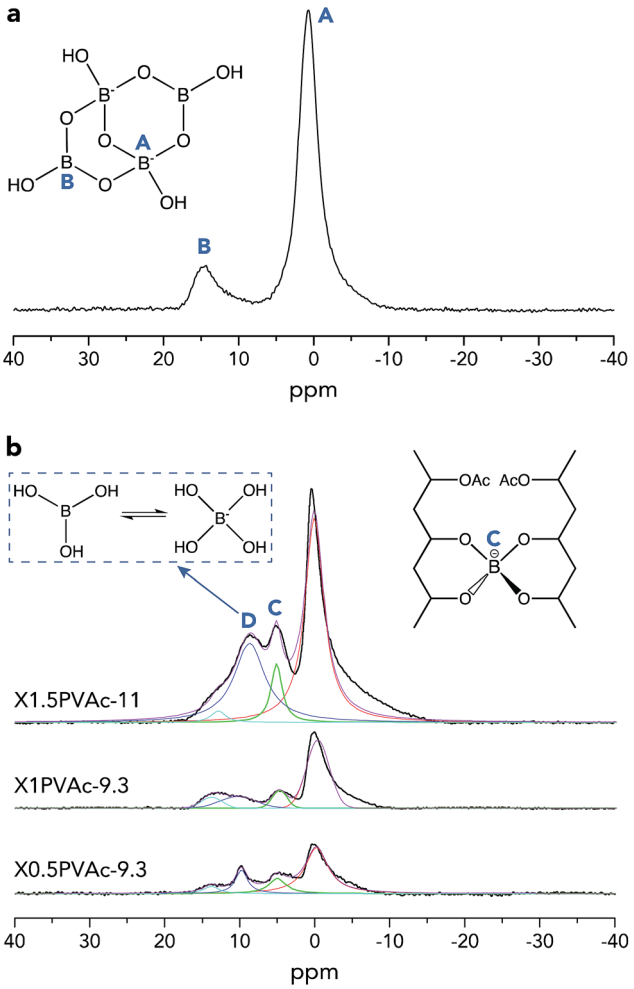

Fig. 2 Single-pulse ^{11}B MAS NMR spectra of a dried borax powder treated at pH 11 (a) and PVAc/borate films (b). The spectra of PVAc/borate were deconvoluted using Lorentzian functions.

Table 3 The crosslinked borate fractions (f_c) and the absolute crosslinked borate content (n_a) of the PVAc/borate samples calculated from the deconvoluted ^{11}B MAS NMR spectra shown in Fig. 2b

Sample coding	f_c (%)	n_a (mol)
X0.5PVAc-9.3	16.9	8.9×10^{-6}
X1PVAc-9.3	9.6	1.0×10^{-5}
X1.5PVAc-11	9.1	1.5×10^{-5}

increase in borax content, the degree of crosslinking in the sample is increased but to a smaller extent at pH > 7; meanwhile, with an increase in pH, the degree of crosslinking in the sample at a constant borax content also increases. This conclusion is in accord with the results reported by Angelova *et al.*[17]

Morphology of latex particles. Fig. 3 compares the morphology of native PVAc and PVAc/borate latex particles. The AFM (Fig. 3a and b) and SEM (Fig. 3c and d) images demonstrate that the average diameter of PVAc-4 latex particles is approximately 79 nm and that of X3PVAc-11 latex particles is

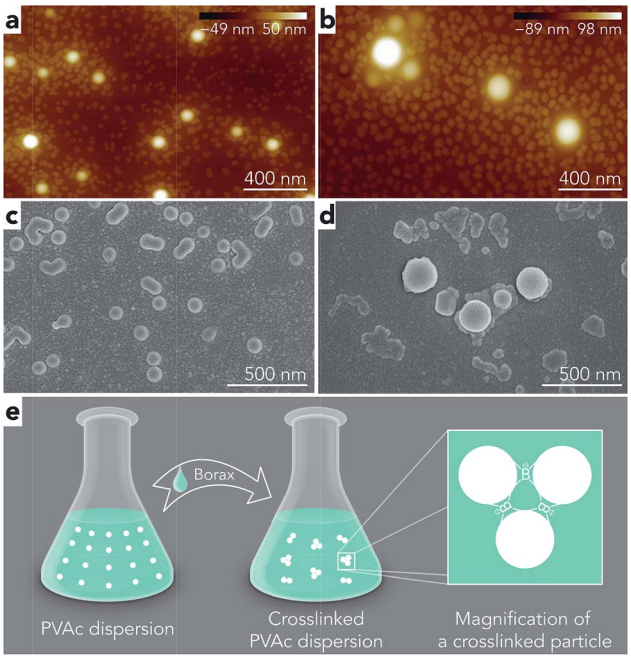

Fig. 3 AFM (height) and SEM images of PVAc-4 (a and c) and X3PVAc-11 (b and d) latex particles and a schematic (e) of one possible mechanism of increasing particle size during the crosslinking reaction.

approximately 180 nm, while there are many small particles on the substrate that could be the docusate sodium salt used as surfactant during the polymerization of vinyl acetate. Both AFM and SEM images show that the size of the PVAc latex particles increases considerably after reacting with the borate additives under alkaline conditions. The possible mechanism of this phenomenon is described in Fig. 3e. When pH > 7, the tetracoordinated borate ions present in the borax solution can react with the partially hydrolysed PVAc and crosslink the PVAc latex particles together to form larger particles. A similar phenomenon has been reported by Song *et al.*, in which the size of polystyrene particles is increased significantly after crosslinking by divinylbenzene.[30]

To further investigate the effect of borate additives on the morphology of PVAc, the particle size results from light scattering measurements performed by a Zetasizer are shown in Fig. 4. First, it can be seen that the sizes of the PVAc-9.3 (100 nm) and PVAc-11 (105 nm) particles are larger than the PVAc-4 (62 nm) particles, which can be attributed to the swelling behaviour of the particles in aqueous medium caused by the presence of more hydrolysed PVAc chains that contain a higher ionic strength and absorb more water molecules.[31] With an increase in borax content, it is interesting to note that the size of the samples treated at pH 4 grows linearly. This is because the borax solution was added into the PVAc latex first, and then, the pH of the dispersion was adjusted during the sample preparation. Therefore, part of the PVAc particles may have already been crosslinked before the pH was tuned to 4. On the other hand, the particle size in the samples treated at pH 9.3 and 11 is also increased, but the rate of this increase is gradually reduced with a further increase in borax content. This is consistent with

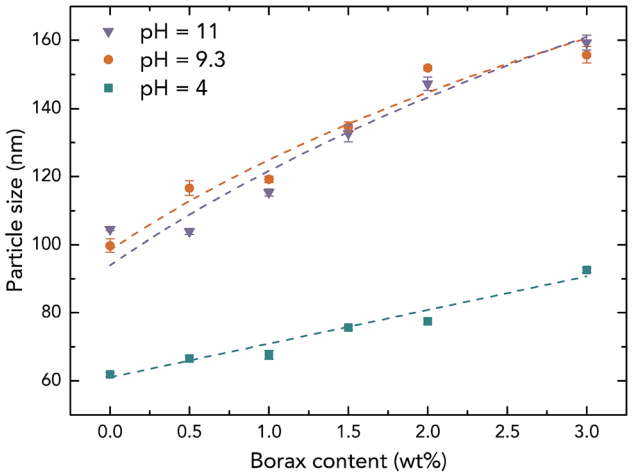

Fig. 4 Particle size of the native PVAc and PVAc/borate latexes prepared with different borax content under various pH levels.

the ^{11}B MAS NMR data (see Table 3), indicating that the degree of crosslinking in the sample follows the same trend under alkaline conditions, because the increased particle size is related to the crosslinking reaction, as explained in Fig. 3e.

However, it can be seen from Fig. 4 that the particle sizes of the samples at pH 9.3 are similar to those at pH 11, although, the samples treated at pH 11 have a larger degree of crosslinking. A possible reason for this is that crosslinking of the PVAc chains may occur within one particle instead of between several particles together that are combined.[32] In addition, by comparing the results from microscopy (Fig. 3) and the light scattering measurements (Fig. 4), one can see that the diameters of particles in samples measured by AFM (horizontal size) and SEM are slightly larger than the particles tested by the Zetasizer. This is because the particles were deformed and became ellipsoids on the substrate during the sample preparation for microscopy due to a low glass transition temperature (close to room temperature) of the PVAc materials,[33] and SEM samples have a tungsten coating layer (thickness is around 3 nm).

Characterization of properties

Mechanical properties. The mechanical properties of the native PVAc and PVAc/borate films were characterized by tensile testing. The results of ultimate strength, elongation at break and elastic modulus of the samples are presented in Fig. 5, and the toughness data are shown in the ESI Table S1.† From

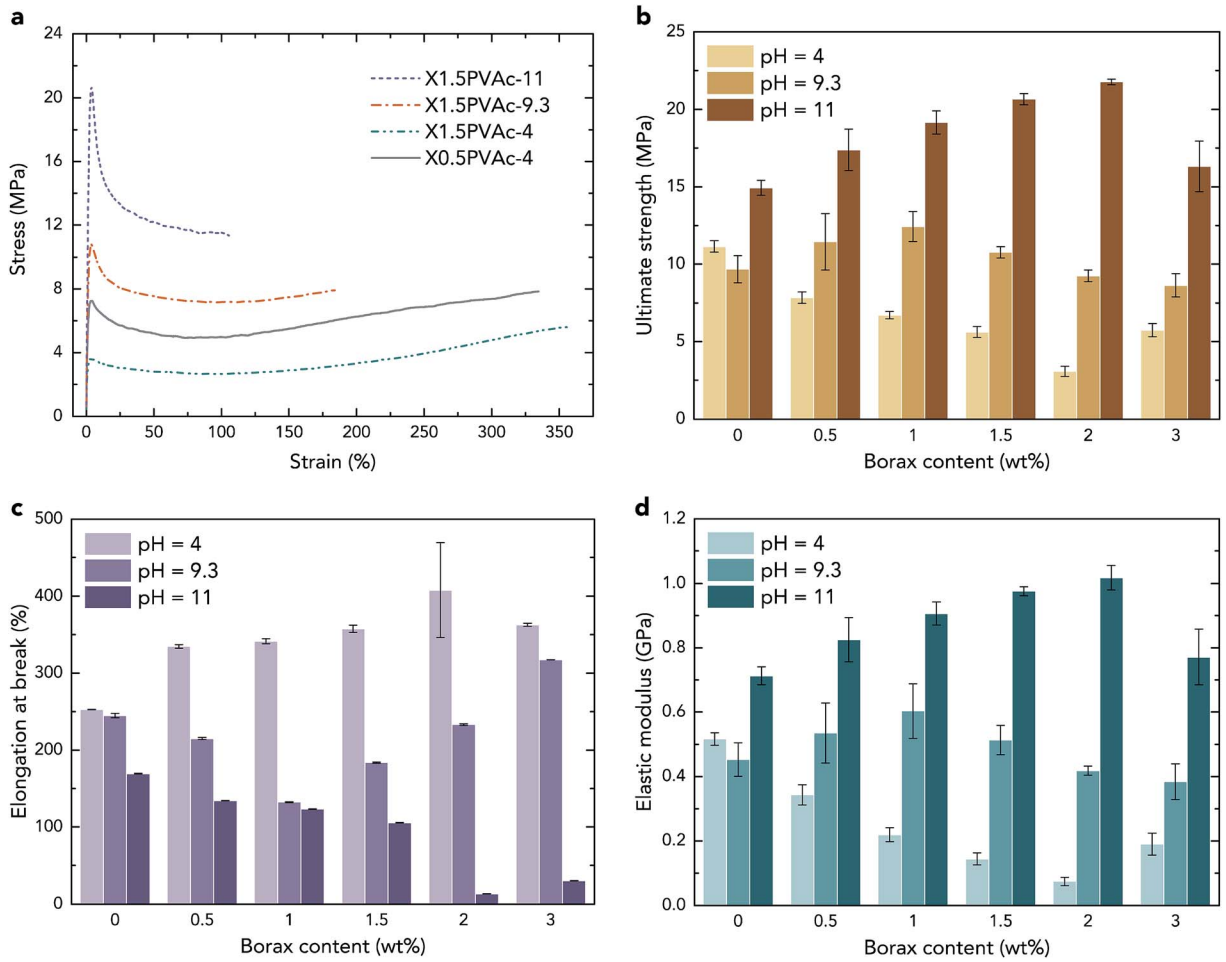

Fig. 5 Stress–strain curves (a), ultimate strength (b), elongation at break (c) and elastic modulus (d) of the native PVAc and PVAc/borate films prepared with various borax content at different pH levels.

Fig. 5a, one can see that with an increase in pH the strength of the samples with 1.5 wt% of borax is enhanced significantly, while the elongation at break is decreased due to an increase in the degree of crosslinking. Meanwhile, X1.5PVAc-4 exhibits a lower strength and a larger elongation at break compared with X0.5PVAc-4, which can be attributed to the plasticizing effect caused by more borate additives. According to the literature, many small molecules containing hydroxyl groups, such as glycerol and sorbitol, have the ability to plasticize PVAc.[34,35] Therefore, boric acid, which is present in all PVAc/borate samples in this study, as confirmed by ^{11}B MAS NMR (region D in Fig. 2b), could also act as a plasticizer.

Consequently, in all PVAc/borate samples, both a crosslinker (tetra-coordinated borate ion) and a plasticizer (boric acid) are present, and they are "competing" with each other. At pH 4, the ultimate strength of the samples shown in Fig. 5b is reduced with an increase in borax content, except for the sample with 3 wt% borax. Although a small amount of PVAc was crosslinked as a result of the sample preparation, as described above, the strength of X3PVAc-4 is still much lower than that of PVAc-4 due to the plasticizing effect. It can also be seen in Fig. 5b that at pH 9.3, with an increase in borax content, the strength of the samples is enhanced and reaches the maximum at 1 wt% borax, and then, it drops down for the samples with >1 wt% borax. Similarly, at pH 11, the ultimate strength reaches the maximum at 2 wt% borax content and then decreases. This is also in accord with the NMR results showing that more borax molecules are converted to the tetra-coordinated borate ions at higher pH levels and form more crosslinks in the samples, providing a higher strength, but the conversion rate declines, and boric acid becomes dominant at high borax concentrations. The elastic modulus of the samples illustrated in Fig. 5d follows exactly the same trend as the ultimate strength, and the elongation at break (Fig. 5c) indicates the opposite trend, which further confirms the "competition" between the crosslinking and plasticizing effects in the samples.

Considering the mechanical properties of the native PVAc samples as reference materials, from Fig. 5b and d, it can be seen that both the strength and the elastic modulus of PVAc-9.3 are slightly lower than those for PVAc-4. A possible reason is that the molecular weight of PVAc is reduced with an increase in pH,[26] which may lead to smaller entanglement of the polymer chains. However, PVAc-11 has a much larger strength and elastic modulus and a lower elongation at break (see in Fig. 5c) compared to those in PVAc-4 and PVAc-9.3. This could be due to a larger number of hydrogen bonds present in PVAc-11, in accord with the NMR data shown in Fig. 1.

Thermal properties. The thermal properties of PVAc are also slightly influenced by borax additives, according to the DSC and TGA results shown in Fig. 6. From Fig. 6a one can see that the glass-transition temperature (T_g) of X2PVAc-11 is somewhat higher than that for PVAc-11, which is caused by the crosslinking effect of borate additives under alkaline conditions. In turn, T_g of X2PVAc-4 is lower than that for PVAc-4, which is attributed to the plasticizing effect under acidic conditions. The glass transition temperatures of all samples measured by DSC are shown in Table 1. It can be seen that, at pH 4, the T_g of the

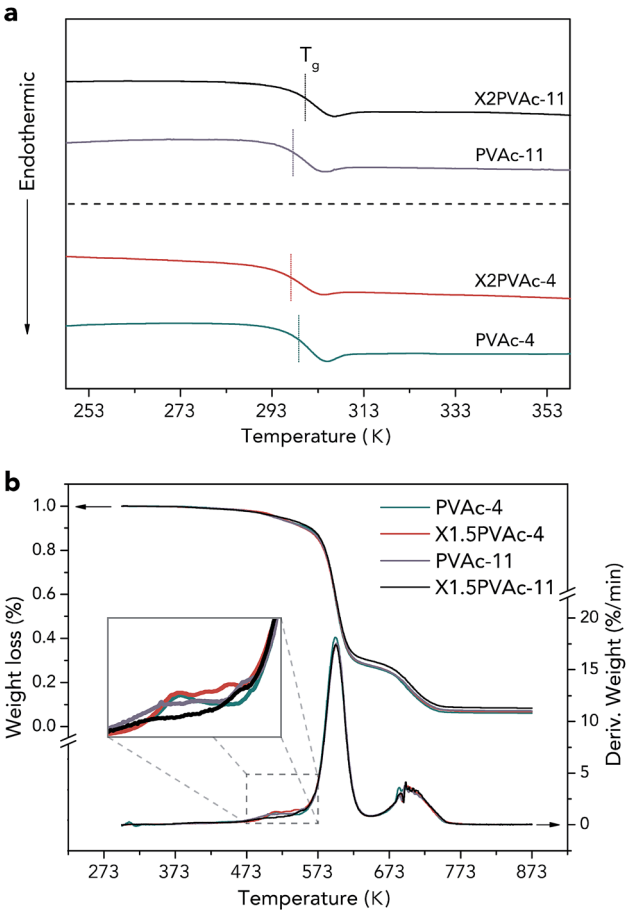

Fig. 6 DSC 2nd heating-run thermograms (a) and TGA curves (b) of native PVAc and PVAc/borate films treated at pH 4 and 11.

samples keeps declining from 298.9 K to 296.8 K with increased borax content; at pH 9.3, it increases to 299.3 K at 1 wt% borax and then decreases, and at pH 11, it reaches the maximum temperature of 300.3 K at 2 wt% borax. The results completely agree with the variations in the mechanical properties of the PVAc/borate samples. Nevertheless, it should be noted that the changes in the T_g caused by borate additives are not significant. One of the possible reasons could be that the samples are only slightly crosslinked due to the low degree of hydrolysis in PVAc based on the NMR data (see Table 2). Meanwhile, the crosslinking and plasticizing effects restrict each other in the samples. Moreover, according to the morphology results shown in Fig. 3, most of the crosslinks in the PVAc/borate samples are consumed to increase the latex particle size instead of forming a 3D network.

The thermal stabilities of the samples were characterized by TGA, and the results are demonstrated in Fig. 6b. The weight loss curves indicate that there are two main PVAc degradation steps: one occurs between 523 K and 623 K and represents deacetylation, and the other occurs between 633 K and 733 K and is caused by chain scission reactions.[36,37] It can also be seen that X1.5PVAc-11 shows a higher stability, especially when the temperature exceeds 613 K, than all the other samples due to the crosslinking effect of borate additives. From the derivative

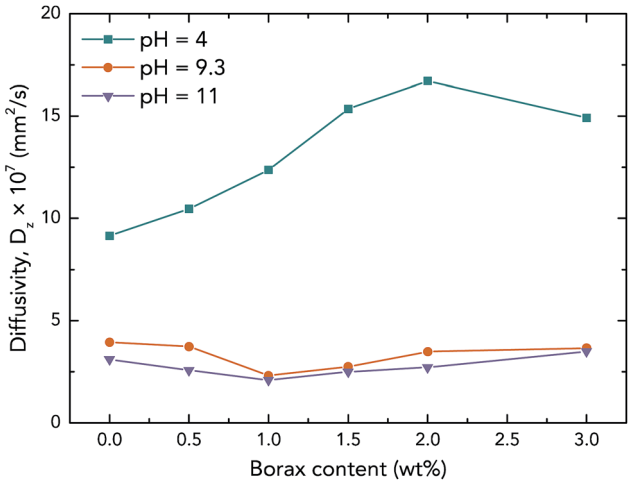

Fig. 7 Diffusivities of native PVAc and PVAc/borate films with different pH and borax concentrations at 90% humidity and 293 K.

weight loss curves, it is obvious that X1.5PVAc-11 starts to degrade at approximately 543 K, while the other samples start to degrade at approximately 493 K.

Moisture absorption behaviour. Fig. 7 reveals the diffusivities of the native PVAc and PVAc/borate films, and their equilibrium moisture content (M_e) values are shown in Table 1. M_e of the samples shows an irregular tendency because it can be influenced by several factors, including the degree of hydrolysis, degree of crosslinking, plasticizer content, and salt.[38] However, in general, one can see that the M_e of the samples is increased with an increase in pH, which is attributed to a larger degree of hydrolysis in PVAc at higher pH, causing water accumulation.[9] In Fig. 7, at pH 4, the diffusivity of the samples is increased with an increase in borax content (except 3 wt% borax). This can be attributed to the plasticizer (boric acid) molecules, which increase the space between the PVAc polymer chains and promote water molecules to pass through the films.[39] When pH is increased to 9.3 or further to 11, the diffusivity of the native PVAc film is reduced considerably due to a larger number of hydroxyl groups hindering diffusion of water molecules and a closer packing of PVAc chains.[40] However, there is no an obvious change in diffusivity of the samples with an increase in the borax content at both pH 9.3 and 11, which indicates that a competition between crosslinking and plasticizing effects could eliminate the variation in moisture absorption behaviour of the PVAc/borate samples.

Conclusions

In summary, both crosslinking and plasticizing effects on PVAc can be provided by borate additives, and the conversion between them depends on the pH during sample preparation. The crosslinking effect dominates under alkaline conditions (pH > 7), and the formation of crosslinks in PVAc/borate materials is confirmed by solid-state ^{13}C and ^{11}B MAS NMR spectroscopy. An increase in the concentration of borate additives at pH 9.3 and 11 is correlated with an increase in the degree of crosslinking in PVAc, and the increase is reduced gradually, which leads to similar variation tendencies in the size of PVAc latex particles and the mechanical and thermal properties of the PVAc/borate films. Plasticizing effects may play a key role at pH 4, and consequently, the strength, elastic modulus, thermal properties and moisture resistance of the PVAc/borate films are reduced with an increase in borate additive content. Because borate additives have generally only been considered crosslinkers in materials, many impacts of these additives may be overlooked. This study provides a different perspective on borate additives.

Acknowledgements

The authors would like to thank Dr Yvonne Aitomäki, Associate Prof. Aji P. Mathew, Dr Christos Nitsos and Prof. Ulrika Rova for technical assistance and valuable discussions. Financial support from the Wallenberg Wood Science Center and Kempe Foundation are greatly appreciated. A "Bruker" NMR spectrometer and Atomic Force Microscopy has been purchased from funds raised by the Kempe Foundation and Luleå University of Technology.

Notes and references

1 M. Amann and O. Minge, in *Synthetic Biodegradable Polymers*, Springer, 2012, pp. 137–172.
2 Y. H. Erbil, *Vinyl acetate emulsion polymerization and copolymerization with acrylic monomers*, CRC press, 2000.
3 Y. Wei, P. Liu, W.-J. Wang, B.-G. Li and S. Zhu, *Polym. Chem.*, 2015, **6**, 2837–2843.
4 E. Bourgeat-Lami, J. Faucheu and A. Noël, *Polym. Chem.*, 2015, **6**, 5323–5357.
5 A. Kaboorani and B. Riedl, *Composites, Part A*, 2011, **42**, 1031–1039.
6 A. Kaboorani, B. Riedl, P. Blanchet, M. Fellin, O. Hosseinaei and S. Wang, *Eur. Polym. J.*, 2012, **48**, 1829–1837.
7 M. W. Perrin, E. W. Fawcett, J. G. Paton and E. G. Williams, *US Pat.*, 2,200,429, 1940.
8 U. Khan, P. May, H. Porwal, K. Nawaz and J. N. Coleman, *ACS Appl. Mater. Interfaces*, 2013, **5**, 1423–1428.
9 A. P. Mathew, G. Gong, N. Bjorngrim, D. Wixe and K. Oksman, *Polym. Eng. Sci.*, 2011, **51**, 2136–2142.
10 G. Gong, J. Pyo, A. P. Mathew and K. Oksman, *Composites, Part A*, 2011, **42**, 1275–1282.
11 G. Gong, A. P. Mathew and K. Oksman, *Polym. Compos.*, 2011, **32**, 1492–1498.
12 H. Ochiai, S. Fukushima, M. Fujikawa and H. Yamamura, *Polym. J.*, 1976, **8**, 131–133.
13 K. Das, D. Ray, N. Bandyopadhyay, A. Gupta, S. Sengupta, S. Sahoo, A. Mohanty and M. Misra, *Ind. Eng. Chem. Res.*, 2010, **49**, 2176–2185.
14 J. Han, T. Lei and Q. Wu, *Cellulose*, 2013, **20**, 2947–2958.
15 S. H. Kim, K. Hyun, T. S. Moon, T. Mitsumata, J. S. Hong, K. H. Ahn and S. J. Lee, *Polymer*, 2005, **46**, 7156–7163.
16 W. Liu, W. Zhang, X. Yu, G. Zhang and Z. Su, *Polym. Chem.*, 2016, **7**, 5749–5762.

17 L. V. Angelova, P. Terech, I. Natali, L. Dei, E. Carretti and R. G. Weiss, *Langmuir*, 2011, **27**, 11671–11682.
18 L. Angelova, M. Leskes, B. Berrie and R. Weiss, *Soft Matter*, 2015, **11**, 5060–5066.
19 I. Natali, E. Carretti, L. Angelova, P. Baglioni, R. G. Weiss and L. Dei, *Langmuir*, 2011, **27**, 13226–13235.
20 S. Geng, M. M.-U. Haque and K. Oksman, *Compos. Sci. Technol.*, 2016, **126**, 35–42.
21 G. W. Barnett and T. T. Chen, *US Pat.*, 4,812,510, 1989.
22 C. R. Morcombe and K. W. Zilm, *J. Magn. Reson.*, 2003, **162**, 479–486.
23 J. G. Cook, *Handbook of Textile Fibres: Natural Fibres*, Elsevier, 1984.
24 N. Asakawa, S. Kuroki, H. Kurosu, I. Ando, A. Shoji and T. Ozaki, *J. Am. Chem. Soc.*, 1992, **114**, 3261–3265.
25 M. J. Sippl, G. Nemethy and H. A. Scheraga, *J. Phys. Chem.*, 1984, **88**, 6231–6233.
26 O. Wheeler, S. Ernst and R. Crozier, *J. Polym. Sci.*, 1952, **8**, 409–423.
27 C. Ho, A. Keller, J. Odell and R. Ottewill, *Colloid Polym. Sci.*, 1993, **271**, 469–479.
28 W. W. Graessley, in *The Entanglement Concept in Polymer Rheology*, Springer, 1974, pp. 1–179.
29 B. Zhou, Z. Sun, Y. Yao and Y. Pan, *Phys. Chem. Miner.*, 2012, **39**, 363–372.
30 J.-S. Song and M. A. Winnik, *Macromolecules*, 2005, **38**, 8300–8307.
31 E. Chatzi and C. Kiparissides, *Chem. Eng. Sci.*, 1994, **49**, 5039–5052.
32 Y. G. Durant, E. J. Sundberg and D. C. Sundberg, *Macromolecules*, 1997, **30**, 1028–1032.
33 D. Vrsaljko, M. Leskovac, S. L. Blagojević and V. Kovačević, *Polym. Eng. Sci.*, 2008, **48**, 1931–1938.
34 P. S. Columbus, *US Pat.*, 06/074,005, 1981.
35 M. G. A. Vieira, M. A. da Silva, L. O. dos Santos and M. M. Beppu, *Eur. Polym. J.*, 2011, **47**, 254–263.
36 B. Rimez, H. Rahier, G. Van Assche, T. Artoos, M. Biesemans and B. Van Mele, *Polym. Degrad. Stab.*, 2008, **93**, 800–810.
37 M. Pracella, M. M.-U. Haque and D. Puglia, *Polymer*, 2014, **55**, 3720–3728.
38 R. W. Korsmeyer and N. A. Peppas, *J. Membr. Sci.*, 1981, **9**, 211–227.
39 N. Gontard, S. Guilbert and J. L. Cuq, *J. Food Sci.*, 1993, **58**, 206–211.
40 R. S. Mahendran, *Characterisation of cross-linking and moisture ingress detection in an epoxy/amine resin using fibre-optic sensors*, University of Birmingham, 2010.